Available online at www.sciencedirect.com
SCIENCE DIRECT®
Journal of Solid State Chemistry 178 (2005) 3624–3630
JOURNAL OF SOLID STATE CHEMISTRY
www.elsevier.com/locate/jssc

A new promising phosphor, $Na_3La_2(BO_3)_3$:*Ln* (*Ln* = Eu, Tb)

Zhihua Li[a,b], Jinghui Zeng[a], Guochun Zhang[c], Yadong Li[a,*]

[a]*Department of Chemistry, Tsinghua University, Beijing 100084, China*
[b]*College of Chemistry, Shandong Normal University, Jinan, Shandong 250014, China*
[c]*Technical Institute of Physics and Chemistry, Chinese Academy of Sciences, P.O. Box 2711, Beijing 100080, China*

Received 22 June 2005; received in revised form 5 September 2005; accepted 9 September 2005
Available online 26 October 2005

Abstract

We present an efficient way to search a host for ultraviolet (UV) phosphor from UV nonlinear optical (NLO) materials. With the guidance, $Na_3La_2(BO_3)_3$ (NLBO), as a promising NLO material with a broad transparency range and high damage threshold, was adopted as a host material for the first time. The lanthanide ions (Tb^{3+} and Eu^{3+})-doped NLBO phosphors have been synthesized by solid-state reaction. Luminescent properties of the *Ln*-doped (*Ln* = Tb^{3+}, Eu^{3+}) sodium lanthanum borate were investigated under UV ray excitation. The emission spectrum was employed to probe the local environments of Eu^{3+} ions in NLBO crystal. For red phosphor, NLBO:Eu, the measured dominating emission peak was at 613 nm, which is attributed to $^5D_0$–$^7F_2$ transition of Eu^{3+}. The luminescence indicates that the local symmetry of Eu^{3+} in NLBO crystal lattice has no inversion center. Optimum Eu^{3+} concentration of NLBO:Eu^{3+} under UV excitation with 395 nm wavelength is about 30 mol%. The green phosphor, NLBO:Tb, showed bright green emission at 543 with 252 nm excited light. The measured concentration quenching curve demonstrated that the maximum concentration of Tb^{3+} in NLBO was about 20%. The luminescence mechanism of *Ln*-doped NLBO (Tb^{3+} and Eu^{3+}) was analyzed. The relative high quenching concentration was also discussed.

Keywords: $Na_3La_2(BO_3)_3$; Luminescence; Solid-state reaction

1. Introduction

Lanthanides have abundant 4*f* electron configurations, when a lanthanide ion is embedded into a host lattice, some well-localized energy states belonging to the $4f^n$ ground configuration and $4f^{n-1}5d$ excited configuration of Ln^{3+} are introduced between the valence and the conduction bands of the host. This will introduce excitation and emission spectra of the transitions occurring between the Ln^{3+} quasi-atomic levels. Lanthanide-doped compounds have played an outstanding role as phosphors in lighting, flat panel displays, optical telecommunication [1], and as the active material in solid-state lasers [2]. It is well known that a fine phosphor, which can be used for illumination or PDP, requires strong UV absorption, high conversion efficiency, wide color gamut and good thermal and chemical stabilities. The properties of the phosphors such as VUV transparency and absorption, optical damage threshold depends strongly on the structure of the host materials [3]. So, the important step is to find good host materials in order to obtained desirable phosphors used for illumination and PDP. However, how to search a good host material is a challenge in the face of thousands upon thousands compounds.

With the development of science and technology, many nonlinear optical crystals have been found for ultraviolet (UV) and vacuum ultraviolet (VUV) generation [4]. It is well known that the requirements for nonlinear optical (NLO) crystals are as follows: wide transparency range for operating wavelength, high laser-induced damage threshold, low material cost, and good chemical stability, etc. These requirements fulfill the preconditions for an ideal UV and VUV phosphors as well. So searching an ideal host for phosphors from NLO crystals may be an efficient way. Among NLO materials, borate has attracted much attention not only owing to their excellent chemical–physical properties and low cost, but also a number of compounds

*Corresponding author. Fax: +86 10 6278 8765.
E-mail address: ydli@mail.tsinghua.edu.cn (Y. Li).

0022-4596/$ - see front matter © 2005 Published by Elsevier Inc.
doi:10.1016/j.jssc.2005.09.018

with different structure can be selected. Furthermore, the B–O covalent bond has no absorption in UV region because of its large covalent bond energy, and the borate always has high damage threshold owing to their wide band-gap of crystal [5]. With the guidance of above, borate NLO materials were adopted as our research emphases.

$Na_3La_2(BO)_3$ (NLBO), is found to be a promising NLO material recently [6]. The NLBO crystal belonged to the orthorhombic system, space group Amm2(#38), with lattice parameters $a = 5.1580(10)$ Å, $b = 11.350(2)$ Å, $c = 7.3230(15)$ Å, $\alpha = \beta = \gamma = 90^\circ$, $Z = 2$, $V = 428.71(15)$ Å^3 (Fig. 1a) [7]. The structure of NLBO crystal could be described as a three-dimensional framework. It was made up of isolated BO_3 triangles held together by the $La(1)O_9$, $Na(1)O_6$, $Na(2)O_8$, and $Na(3)O_6$ polyhedron. Its excellent performances such as wide transparency range (200–2500 nm), high damage threshold and chemical and physical stabilities suggest that it may be a good host material for phosphors. Furthermore, the structure of the compound will be maintained when the La^{3+} ion is replayed by other RE^{3+} owing to their smaller radius compared with that of lanthanum. Until to now, the study about lanthanide-doped NLBO has not been reported to our knowledge. NLBO has many advantages such as environmental benignity, potential low-cost synthesis, and high thermal stability, etc. So, NLBO intrigues us to investigate the properties of RE^{3+}-doped NLBO phosphors as a good potential host.

It is well known that the commonly used doping ions are Eu^{3+} and Tb^{3+} because of their high luminescence intensity in numerous phosphors attribute to the abundant d–f electron transitions. In particular, the Eu^{3+} ion provides a convenient approach to the study of the luminescence properties of rare-earth ions. First, the luminescence line spectrum is relatively easy to analyze since the strongest transitions originate from an energy state not split by the crystal field. Secondly, the study about some particular features of the energy level scheme of this ion, such as the even number of electrons and large energy gap between the ground state ^7F septuplet and the excited

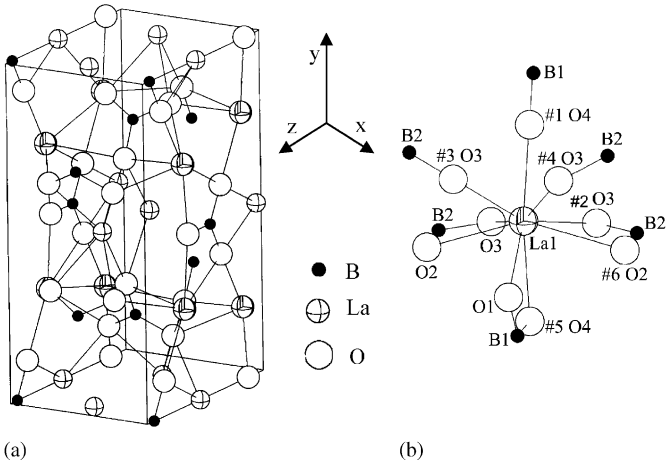

Fig. 1. (a) The structure of NLBO, (b) the structure of LaO_9 group.

levels is a representative problem. Consequently, the Eu^{3+} ion has been extensively used to probe the local environment of dopant sites.

In our present work, we synthesized NLBO:Ln^{3+} ($Ln = Tb^{3+}$, Eu^{3+}) phosphors by solid-state reaction. The luminescent ions corresponding environment in NLBO crystal lattice was analyzed using Eu^{3+} ions as a probe. The luminescent properties of NLBO:Ln^{3+} ($Ln = Tb^{3+}$, Eu^{3+}) phosphor, the luminescence mechanism, and the concentration quenching of Ln^{3+}-doped NLBO were also investigated.

2. Experiment

In this work, phosphor samples of NLBO:Ln^{3+} were prepared by using solid-state reaction techniques. The chemical equation can be expressed as follows:

$$6H_3BO_3 + xEu_2O_3 + 2(1-x)La_2O_3 + 3Na_2CO_3 = 2Na_3La_{2(1-x)}Eu_{2x}(BO_3)_3 + 3CO_2 + 9H_2O$$

$$3Na_2CO_3 + 2(1-x)La_2O_3 + 6H_3BO_3 + x/2Tb_4O_7 = 2Na_3La_{2(1-x)}Tb_{2x}(BO)_3 + 3CO_2 + 9H_2O + x/4O_2$$

All of the used reagents were analytical purity.

Preparation of the red phosphors was carried out in the following steps. The analytical grade Eu_2O_3, Na_2CO_3, La_2O_3, and H_3BO_3 of different weight ratio were weighed, mixed homogeneously in an agate mortar, and then packed into a crucible. The temperature was raised slowly to 500 °C in order to avoid ejection of powdered raw material from the crucible due to the decomposition of H_3BO_3 and Na_2CO_3. After preheating at 500 °C for 10 h in a muffle furnace, the products were cooled to room temperature, and ground up again; the mixture was sintered at 850 °C for 24 h, and then cooled to room temperature. The purity of sample was characterized by X-ray powder diffraction. The synthesis method of green phosphors was the same as that of red phosphors except that Tb_4O_7 was used instead of Eu_2O_3.

$Y_{1.8}O_3$:$Eu_{0.2}$ was synthesized by solid-state reaction at 1250 °C for 5 h in order to compare with NLBO:Eu.

The phase identification was carried out by powder X-ray diffraction using a Brucker D8-advance X-ray Diffractometer with Cu $K\alpha$ radiation ($\lambda = 1.5418$ Å), the operation voltage and current keeping at 40 kV and 40 mA, respectively. The 2θ range used was from 10° to 70° in steps of 0.02° with a count time of 0.2 s. The samples with different Eu^{3+} concentration were prepared by above synthesis method. Fluorescent spectra were recorded with a Hitachi F-4500 Fluorescence Spectrophotometer. Scan speed was 15 nm/min. PMT voltage was 700 V. Scanning electron microscopy (JSM6301F) was used for the observation of particle morphology. All samples were measured at the same condition.

3. Results and discussion

In order to compensate for the volatilization of boron oxide at high temperature, H_3BO_3 should be excess about 1–5% during the synthesis process.

The synthesis of purity phase NLBO:Eu is very important in order to determine the exact local symmetry of active ions in NLBO using Eu^{3+} as a fluorescent probe. The primarily impurity is $LaBO_3$ during the synthesis process. $LaBO_3$ would be created easily if excess H_3BO_3 is up to of 5%. Reaction temperature is another considerable factor for obtaining the pure phase NLBO:Eu. Reaction progress would be incompletely if temperature is lower than 800 °C, and the prepared phosphors would be decomposed partially if temperature exceeds 950 °C. The experiments show that the optimum range of reaction temperature is about from 800 to 900 °C. The phase transition phenomenon between NLBO and $LaBO_3$ was observed under 800–900 °C. NLBO was obtained when $LaBO_3$, H_3BO_3 and Na_2CO_3 with molar ratio 4:6:3 were mixed thoroughly, and then heated at 850 °C for 20 h. So, the synthesis of pure phase NLBO was determined by the moderate initial charges ratio.

It is well known that rare earth ions have similar radius, coordination structure and physical-chemical properties. When one La^{3+} is replaced by Eu^{3+} or Tb^{3+}, the crystal structure does not change dramatically. Fig. 2 shows the XRD patterns of the as-prepared samples. The effective radius of La^{3+}, Eu^{3+} and Tb^{3+} in LnO_9 group are 121.6, 112.0 and 109.5 pm, respectively [8]. The lattice parameters of NLBO will reduces gradually with doping concentration of Eu^{3+} or Tb^{3+} increasing. The varieties of unit cell constant of NLBO-*Ln* were calculated and the results were given in Table 1. As can be seen from the XRD patterns, all of the diffraction peaks are shifted to high angle slightly along with the increasing of Eu^{3+} or Tb^{3+} doping levels.

3.1. NLBO:Eu^{3+} Phosphor

The strong red emission peak in the emission spectrum (Fig. 3) suggested that the Eu^{3+}-doped NLBO phosphors were synthesized successfully. The emission spectra of NLBO:Eu consist of lines mainly located in the wavelength range from 570 to 705 nm. These lines correspond to transitions from the excited state $^5D_0$ to the ground state ^7F_J ($J = 0, 1, 2, 3, 4$) of the $4f^6$ configuration of Eu^{3+}, as marked in Fig. 3. Luminescence originating from transitions between 4*f* levels is predominant due to electric dipole or magnetic dipole interactions [9]. In accordance with Judd–Ofelt theory, transitions to even *J*-numbers have much higher intensity than those to corresponding neighboring odd *J*-numbers. The intensity of electric dipole transitions depends strongly on the site symmetry in a host crystal. Magnetic dipole *f*–*f* transitions are not affected much by the site symmetry because they are parity-allowed. The intensities of different $^5D_0 \rightarrow {}^7F_J$ transitions and the splittings of these emission peaks depend on the local

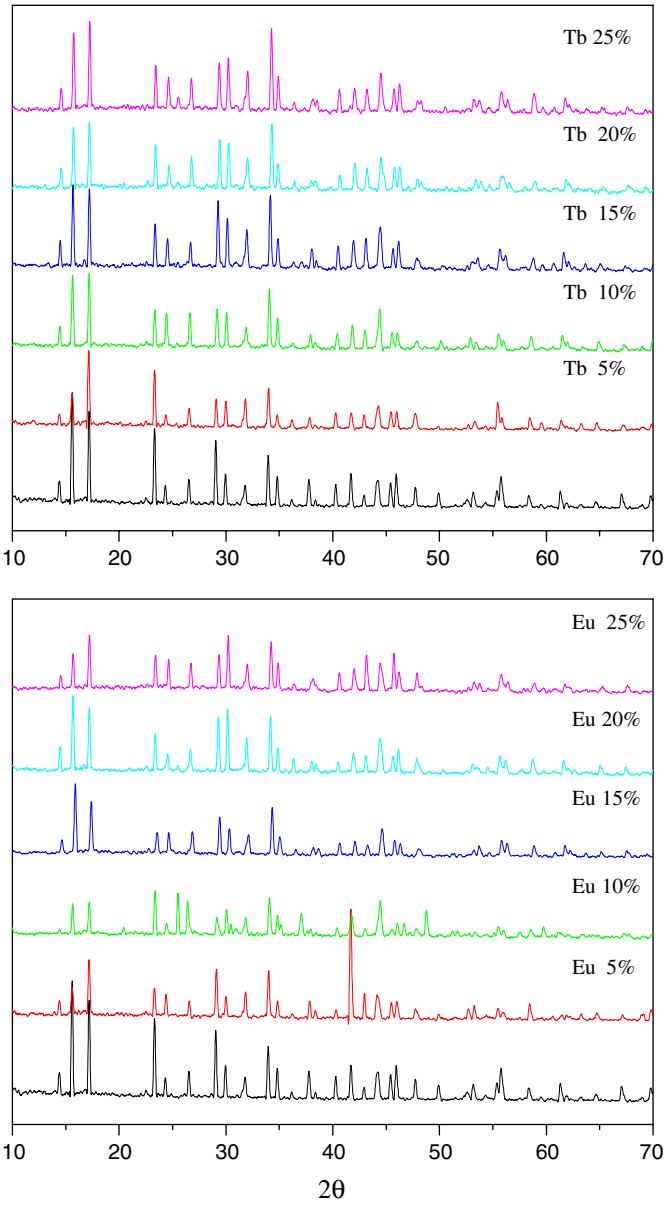

Fig. 2. XRD pattern of NLBO:*Ln* (*Ln* = Eu, Tb).

symmetry of the crystal field of Eu^{3+} ion. If Eu^{3+} occupies an inversion symmetry site in the crystal lattice, the orange-red emission, magnetic dipole transition $^5D_0 \rightarrow {}^7F_1$ (around 590 nm) is the dominant transition. On the contrary, if Eu^{3+} does not occupy the inversion symmetry site, the electric dipole transition $^5D_0 \rightarrow {}^7F_2$ (around 610–620 nm) is the dominant transitions. In Fig. 4, as can be seen that the strong red emission lines at 612 nm originating from the electric dipole transition $^5D_0 \rightarrow {}^7F_2$ are the dominant bands in the measured spectrum. So the site in NLBO occupied by Eu^{3+} has no inversion symmetry. The emission peak at around 580 nm is attributed to the $^5D_0 \rightarrow {}^7F_0$ transition. It is known that the $^5D_0 \rightarrow {}^7F_0$ transition is very sensitive to the local environment of Eu^{3+} ion. According to the parity selection rule, optical transitions between the $^5D_0$ and $^7F_0$ levels ($\Delta J = 0$, and from $J = 0$ to 0) are strictly forbidden

Table 1
Unit cell variety of NLBO with doped-Eu^{3+} or -Tb^{3+} concentration increasing

	a (Å)	b (Å)	c (Å)
Tb (%)			
0	5.1580	11.3502	7.3230
5	5.1508	11.3112	7.2893
10	5.1291	11.2865	7.2601
15	5.1328	11.2503	7.2482
20	5.1279	11.2358	7.2054
25	5.1235	11.2314	7.2292
Eu (%)			
0	5.1580	11.3502	7.3230
5	5.1549	11.3503	7.2778
10	5.1404	11.3027	7.2947
15	5.1323	11.2553	7.2556
20	5.1210	11.2350	7.2299
25	5.1063	11.2236	7.2281

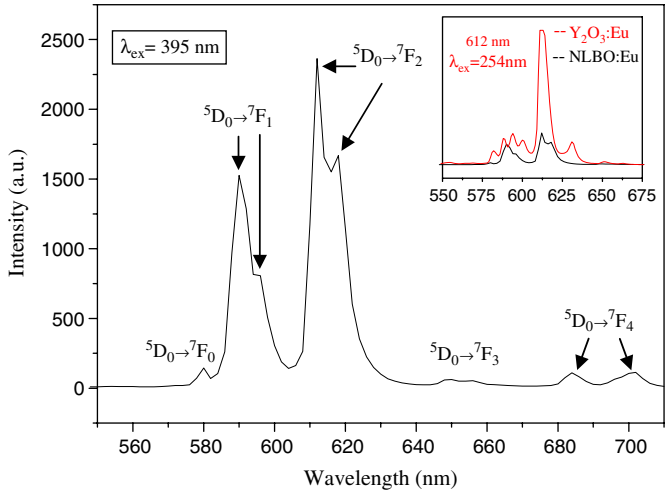

Fig. 3. The emission spectrum of NLBO:Eu (30 %) EX slit: 2.5 nm; EM slit: 2.5 nm.

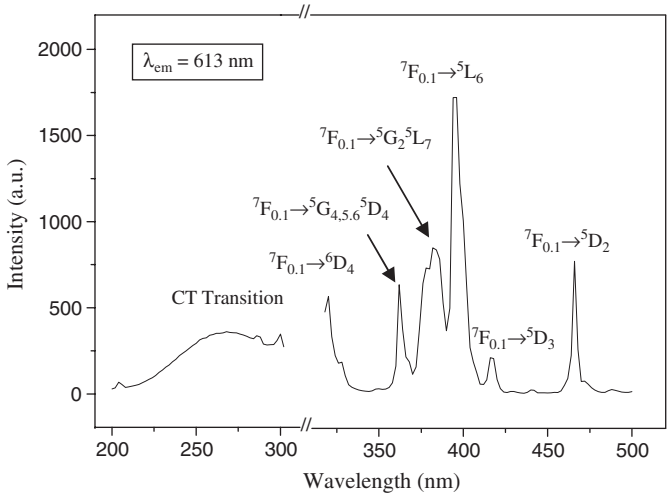

Fig. 4. The excitation spectrum of NLBO:Eu (30 %) EX slit: 2.5 nm; EM slit: 2.5 nm.

if the Eu^{3+} ion occupies an inversion symmetry site in the crystal lattice. However, if the site occupied by Eu^{3+} has no inversion symmetry—C_s, C_n, or C_{nv} symmetry, the uneven crystal field components can lead to the mixing of opposite parity states into the $4f^n$ configuration levels. The $^5D_0 \rightarrow {}^7F_0$ transition (electric dipole transition) become no strictly forbidden and gives rise to weak lines in the emission spectra. The $^5D_0 \rightarrow {}^7F_0$ transition has only one emission peak when Eu^{3+} occupies one lattice site. In the other words, the number of emission peaks equal to that of the lattice sites occupied by Eu^{3+}. As depicted in Fig. 2, there is one emission peak at around 580 nm, which indicated Eu^{3+} occupied only one lattice site in NLBO crystal. So, it is affirmed that the local symmetry of Eu^{3+} belongs to one of the symmetry—C_s, C_n, and C_{nv}. It is reported that $Na_3La_2(BO_3)_3$ crystals belong to C_{2v} point group, the coordination number of La^{3+} is 9. The structure of LaO_9 group is depicted in Fig. 1b. There is a 2-fold axis in LaO_9 group. Combined with the experiment data, we conclude that the local symmetry of Eu^{3+} in NLBO may be C_2.

The measured excitation spectrum of NLBO:Eu was showed in Fig. 4. The excitation data of the main red fluorescence ($\lambda_{em} = 613$ nm) was recorded from 200 to 500 nm. The broadband centered at 287 nm is attributed to a charge-transfer (CT) transition, which occurs by electron delocalization from the filled $2p$ shell of the O^{2-} to the partially filled $4f$ shell of Eu^{3+}. Several intense and sharp lines were exhibited in the range of 300–500 nm in Fig. 4. These correspond to the direct excitation of the europium ground state into higher excited states of the europium f-electrons. The sharp absorption lines attributed to the bands of f–f transitions of Eu^{3+}, whose positions agree with other Eu^{3+}-doped materials [10]. The most intense peak at about 395 nm corresponding to the $^7F_{0,1} \rightarrow {}^5L_6$ transition.

In Fig. 3, the inset was the emission spectrum of Y_2O_3:Eu and NLBO:Eu. As can be seen, the red light intensity of NLBO:Eu ($\lambda_{ex} = 395$ nm) was about 1/4 that of Y_2O_3:Eu ($\lambda_{ex} = 254$ nm).

The composition with the highest luminescence intensity was determined by varying the europium content of NLBO phosphors (Fig. 5 right). The quantum yield shows a maximum at a doping level of about 30 mol% europium and then decreases at higher europium concentrations. This partial quenching of the luminescence at high europium concentrations is a typical property of lanthanide-doped systems and is observed if the mean distance between neighboring europium ions decreases below a critical value.

3.2. NLBO:Tb^{3+} phosphor

The excitation and emission spectra of $Na_3La_{1.82}Tb_{0.18}(BO)_3$ and Zn_2SiO_4:Mn (commercial phosphor) are showed in Fig. 6. The excitation spectrum of $Na_3La_{1.82}Tb_{0.18}(BO)_3$ (left- hand side of figure) is taken at an emission wavelength of 545 nm, its emission spectrum (right-hand

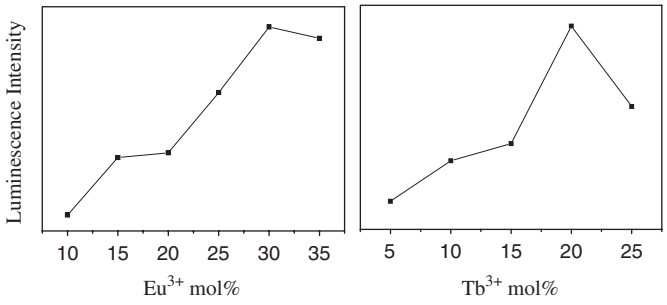

Fig. 5. Concentration quenching curves of Eu^{3+} and Tb^{3+}, respectively.

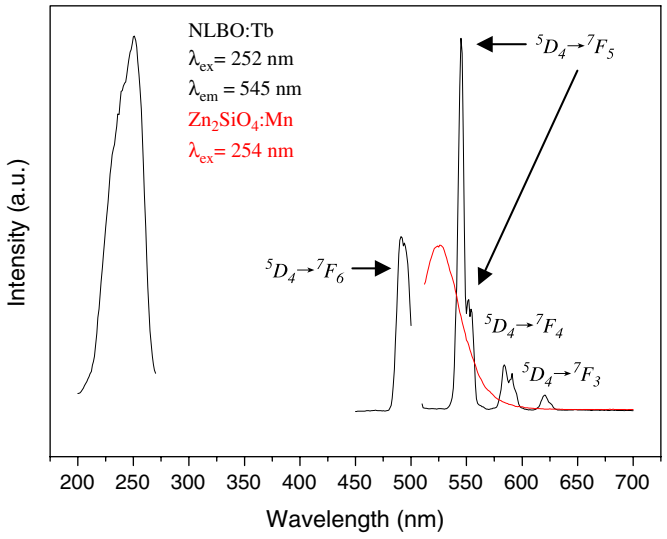

Fig. 6. Excitation and emission spectrum of NLBO:Tb and emission spectrum of Zn_2SiO_4:Mn EX slit: 1.0 nm; EM slit: 1.0 nm.

side of figure) is taken with an excitation wavelength of 252 nm. It is known that Tb^{3+} ion has a reasonable green emission resulted from the $^5D_4 \rightarrow {}^7F_J$ ($J = 6, 5, 4, 3$) transition [11] between 450 and 700 nm. In emission spectrum, there are seven peaks locating at 490, 545, 552, 554, 583, 591, and 621 nm, which are associated with the transition from $^5D_4 \rightarrow {}^7F_6$ (490 nm), $^5D_4 \rightarrow {}^7F_5$ (545, 552 and 554 nm), $^5D_4 \rightarrow {}^7F_4$ (583 and 591 nm), and $^5D_4 \rightarrow {}^7F_3$ (621 nm) respectively. The red curve in Fig. 6 was the emission spectrum of $Na_3La_{1.82}Tb_{0.18}(BO)_3$ and Zn_2SiO_4:Mn (commercial phosphor), it showed that the green light intensity of NLBO:Tb was about two times that of Zn_2SiO_4:Mn under the nearly same excitation wavelength.

In general, the luminescent intensity is proportional to the concentration of activators which could be excited by incident photons. As increasing the concentration of the activator, however, the emission intensity is saturated and begins to decrease at over a critical quenching concentration. Fig. 5 (left) shows the concentration quenching curve of Tb^{3+} ions doped in $Na_3La_2(BO)_3$. The phosphor showed the strongest green emission intensity when Tb^{3+} ion doping concentration increasing to 20 mol%.

Herein we discuss the excellent luminescence properties of $Na_3La_{1.8}Tb_{0.2}(BO)_3$ in detail. When excited by a normal continuous wave Xe source, using the minimum excitation slit and 700 V PMT Voltage, the emitting bright green light with unexpectedly high fluorescent intensity was observed. In the emission spectrum, we also noticed that there are six peaks in the measured range from 510 to 700 nm. As a green phosphor, the intensity of orange emission (583 and 591 nm) of as-prepared phosphors is very weak than that of the green one (545, 552, and 554 nm), leading to a good monochromaticity. The position of the broad excitation peak at around 252 nm meeting with 253.7 nm UV irradiation of free-Hg light leads to the efficiency and completely absorption the irradiation energy of Mercury-free fluorescence lamp (Fig. 7).

Comparing the emission spectrum of NLBO:Eu with that of NLBO:Tb (Fig. 8), we noticed that the intensity of green emission peak (545 nm) is about 12 times of the main peak (613 nm) of the europium-doped sample. Its difference in intensity may be related to the different electronic structures of the doping rare-earth ions and their interaction with the host lattice. Because all samples were synthesized under the same condition and their crystallinity of as-prepared phosphors were almost identical.

This phenomenon should be explained from the excitation mechanisms of both samples. In Fig. 4, the observed excitation bands between 300 and 500 nm attribute to the

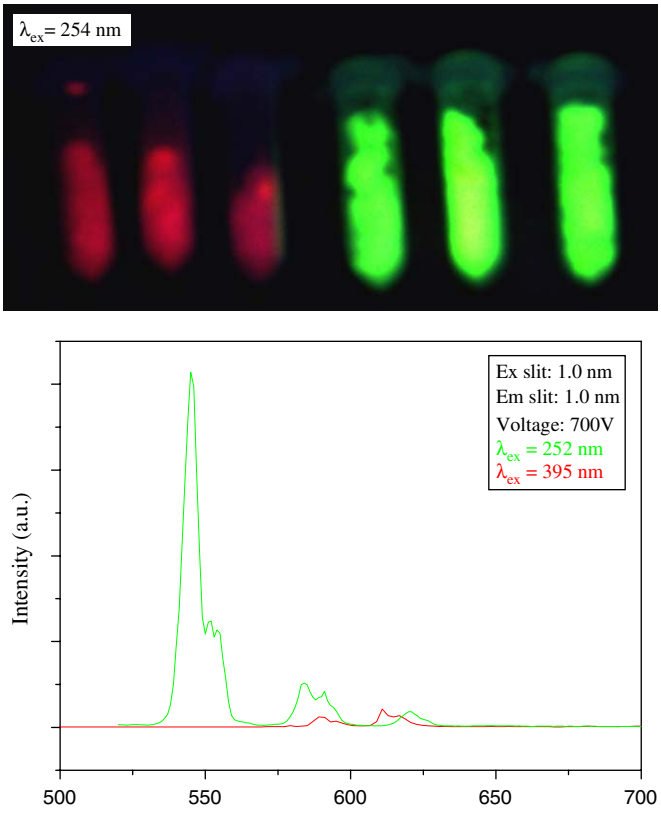

Fig. 7. Comparison the emission spectrum of NLBO:Eu (5%) with that of NLBO:Tb (5%).

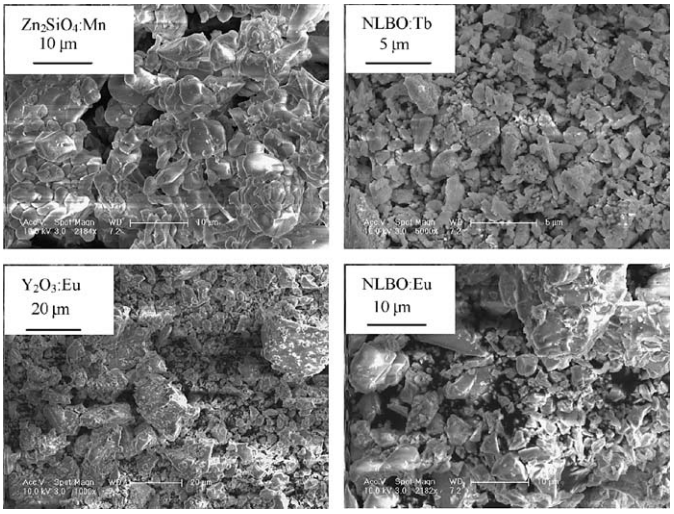

Fig. 8. SEM pictures of phosphors.

$4f \rightarrow 4f$ intra-configuration transitions, which are generally electric dipolar transitions forbidden by the parity selection rules and forced by the crystal field configuration mixing. In Fig. 6, the broad and intense band was centered at 252 nm under 545 nm excited light sources for $Na_3La_{1.8}Tb_{0.2}(BO)_3$ phosphors. The broad and intense excitation peak corresponds to the inter-configuration transitions from $4f^8$ to $4f^7 5d^1$ levels [12], which is caused by the dipolar electric parity allowed transitions. Furthermore, the f–d transition is crystal-field sensitive due to the large radial extension of $5d$ orbitals, and the energy transfer process between the $5d$ and $4f$ levels may be assisted by host phonons [12]. So, the bands of f–f transitions of Eu^{3+} exhibited weaker and shaper absorption peaks compared to the f–d transition peaks.

In experiments, we also noticed that the quenching concentration of active ions in NLBO:Ln ($Ln = Tb^{3+}$, Eu^{3+}) was very high, this was related to the structure of NLBO. The nearest La^{3+}– La^{3+} distance and second nearest La^{3+}–La^{3+} in NLBO reported were 3.755 Å and 4.842 Å, respectively [6]. The interacted effect of La^{3+}–La^{3+} was reduced owing to the relatively large distance between La^{3+}–La^{3+}. So, the probability of energy transfer between Ln^{3+}–Ln^{3+} was also decreased when La^{3+} was replaced by active ions such as Eu^{3+} or Tb^{3+}, the quenching concentration of active ions was relatively increased.

SEM pictures of Zn_2SiO_4:Mn, Y_2O_3:Eu, NLBO:Tb and NLBO:Eu are given in Fig. 8. As can be seen, the particle size distribution and surface of Zn_2SiO_4:Mn are relatively narrow and smooth than that of NLBO:Tb and NLBO:Eu, respectively. It is well known that the well-crystallined and the morphology of the particles are the important factors for increasing brightness of phosphors. In our further work, sol–gel method and the way using feasible flux in solid-state synthesis process will be employed to improve the crystal morphology.

With the development of plasma display panel (PDP) and VUV spectroscopy, lanthanide-doped borate phosphors have been attracted much attention owing to its excellent merits such as low cost, high luminescent efficiency excited by UV light and, etc. Just as well-known nowadays used phosphors for PDP: green phosphor $GdMgB_5O_{10}$:CeTb (CBT) and (Y,Gd)BO_3:Tb, and red phosphor (Y,Gd)BO_3:Eu [13], the as-prepared NLBO:Ln ($Ln = Tb^{3+}$, Eu^{3+}) phosphors may be a candidate for PDP, and before this, the VUV excitation and emission spectra should be measured.

It is well known that the well-crystallined and the morphology of the particles are the important factors for increasing brightness of phosphors. In our further work, sol–gel method and the way using feasible flux in solid-state synthesis process will be employed to improve the crystal morphology.

4. Conclusions

A new phosphor, NLBO:Ln ($Ln = Tb^{3+}$, Eu^{3+}), was designed and synthesized by solid-state reaction for the first time. The excitation and emission spectra of the as-prepared phosphors were measured. In the excitation spectrum curve, the most intense peak at about 395 nm corresponded to the $^7F_{0,1} \rightarrow {}^5L_6$ transition and a wide band around 287 nm attributed to a CT transition. The predominating emission peak was at 613 nm, which indicated that the local environments of Eu^{3+} ions in NLBO crystal had no inversion symmetry. We conclude from the experiments data that the Eu^{3+} ions may possess C_2 symmetry. The maximum Eu^{3+}-doped concentration in NLBO under UV excitation with 395 nm wavelength was about 30% (molar ratio). The strong absorption band in the excitation spectrum was at about 252 nm, and its intense green emission peak was at about 545 nm. The measured optimum doped concentration of Tb^{3+} was about 20% in molar ratio. In view of the luminescent characteristics of the prepared phosphors, NLBO:Ln ($Ln = Tb^{3+}$, Eu^{3+}) may be a promising phosphors candidates for high efficiency fluorescence lamps and other related application.

Acknowledgment

This work was supported by NSFC (90406003, 20151001), the Foundation for the Author of National Excellent Doctoral Dissertation of P.R. China and the state key project of fundamental research for nanomaterials and nanostructures (2003CB716901).

References

[1] (a) M.J. Denjake, B. Samson, Mater. Res. Soc. Bull. 8 (1999) 39;
(b) Y.C. Yan, A.J. Faber, H. Waal, P.G. Kik, A. Polman, Appl. Phys. Lett. 71 (1997) 2922;

(c) H. Giesber, J. Ballato, G. Chumanov, J. Kolis, M. Dejneka, J. Appl. Phys. 93 (2003) 8987;
(d) G.S. Yi, H.C. Lu, S.Y. Zhao, Y. Ge, W.J. Yang, D.P. Chen, L.H. Guo, NanoLetters 4 (2004) 2191.
[2] (a) E. Downing, L. Hesselink, J. Ralson, R. MacFarlane, Science 272 (1996) 1185;
(b) A. Braud, S. Girard, J.L. Doualan, M. Thuau, R. Moncorge, A.M. Tkachuk, Phys. Rev. B 61 (2000) 5280;
(c) H.R. Xia, L.X. Li, H.J. Zhang, X.L. Meng, L. Zhu, Z.H. Yang, X.S. Liu, J.Y. Wang, J. Appl. Phys. 87 (2000) 269.
[3] (a) G. Chadeyron, M. El-Ghozzi, R. Mahiou, A. Arbus, J.C. Cousseins, J. Solid State Chem. 128 (1997) 261;
(b) Z. Yang, M. Ren, J.H. Lin, M.Z. Su, et al., Chem. J. Chin. Univ. 21 (2000) 1339;
(c) Z.H. Li, Z.H. Lin, Y.C. Wu, et al., Chem. Mater. 16 (15) (2004) 2906.
[4] (a) C. Chen, B. Wu, A. Jiang, G. You, Sci. Sin. B 7 (1984) 598;
(b) C. Chen, Y. Wu, A. Jiang, G. You, R. Li, S. Lin, J. Opt. Soc. Am. B 6 (1989) 616;
(c) L. Mei, Y. Wang, C. Chen, B. Wu, J. Appl. Phys. 74 (1993) 7014;
(d) C. Chen, Y. Wang, B. Wu, K. Wu, W. Zeng, L. Yu, Nature (London) 322 (1995) 373;
(e) Y. Wu, T. Sasaki, S. Nakai, A. Yokotani, H. Tang, C. Chen, Appl. Phys. Lett. 62 (1993) 2614.
[5] C. Chen, N. Ye, et al., Adv. Mater. 11 (13) (1999) 1071.
[6] G. Zhang, Ph.D. Thesis, University of Science and Technology of China, 2001.
[7] (a) G. Zhang, Y. Wu, P. Fu, et al., Chem. Lett. 5 (2001) 455–457;
(b) J. Mascetti, C. Fouassier, P. Hagenmuller, J. Solid State Chem. 50 (1983) 204.
[8] R.D. Shannon, Acta. Crystallogr. A 32 (1976) 751.
[9] (a) G. Blasse, B.C. Grabmaier, Luminescence Materials, Springer, New York, 1994, p. 22;
(b) S. Shionoya, W.M. Yen, Phosphor Handbook, CRC Press, Boca Raton, 1999, p. 190;
(c) S.-I. Mho, J.C. Wright, J. Chem. Phys. 77 (1982) 1183;
(d) B.R. Judd, Phys. Rev. 127 (1962) 750;
(e) G.S. Ofelt, J. Chem. Phys. 37 (1962) 511.
[10] (a) R. Balda, J. Fernández, J.L. Adam, M.A. Arriandiaga, Phys. Rev. B 54 (1996) 12076;
(b) K. Riwotzki, H. Meyssamy, A. Kornowski, M. Haase, J. Phys. Chem. B 104 (2000) 2824;
(c) H. Song, B. Chen, H. Peng, J. Zhang, Appl. Phys. Lett. 81 (2002) 1776–1778;
(d) R.X. Yan, Y.D. Li, Adv. Funct. Mater. 15 (5) (2005) 763–770.
[11] M. Zawadzki, D. Hreniak, J. Wrzyszcz, W. Mista, H. Grabowska, O.L. Malta, W. Strek, Chem. Phys. 291 (2003) 275.
[12] J.C. Krupa, M. Queffelec, J. Alloy Compd. 250 (1997) 287.
[13] (a) A.W. de Jager-Veenis, A. Bril, J. Electrochem. Soc. 123 (1976) 1253;
(b) J. Koike, T. Kojima, R. Toyonaga, A. Kagami, T. Hase, S. Inaho, J. Electrochem. Soc. 126 (1979) 1008.